Effect of edge length and wettability on droplet impact onto a stand-alone cubic pillar

A. K. Geppert*[1], P. Foltyn[1], B. Weigand[1]

[1]Institute of Aerospace Thermodynamics, University of Stuttgart, Germany
*Corresponding author: anne.geppert@itlr.uni-stuttgart.de

Abstract
Droplet impact on dry, structured surfaces is ubiquitous in nature and technology, e.g., in soil erosion, spray painting, anti-icing coatings or self-cleaning surfaces. These applications also depend on the wetting behaviour of the surface. To gain a better understanding of the complex interplay between surfaces structure and wettability, a single droplet impact onto a stand-alone cuboid is investigated. In this paper, we present the results of an investigation where the edge length of the cubic pillar is varied between 1 mm and 2.4 mm as well as its surface wettability (full wetting to almost non-wetting conditions). The parameter variation also includes multiple droplet diameters, impact velocities and two fluids, namely water and isopropanol. The droplet impact process is visualized with the multi-perspective experimental facility [2], that employs the total internal reflection-configuration to resolve the liquid-solid contact area. Our investigation revealed that an increase in pillar size with respect to the droplet diameter leads to a change in spreading morphology from ground spreading to umbrella spreading. Ground spreading is characterized by the liquid flowing around the pillar and along the surrounding substrate, while umbrella spreading refers to the formation of the liquid lamella in mid-air. Furthermore, the spreading shape changes from circular to rectangular, which promotes the filament formation. The wettability of the target surface mainly affects the spreading at later times and the retraction behaviour of the liquid.

Keywords
Droplet dynamics, dry structured surface, experiments, surface wettability, surface topography

Introduction

Many processes in technology and nature, e.g. spray painting, self-cleaning surfaces or soil erosion, comprise on some level the interaction of a single droplet with a dry, structured surfaces. These processes usually also depend on the wetting behaviour of the surface. Spray painting, e.g., requires a high wettability of the surface to achieve an even distribution of the paint, while self-cleaning surfaces repel liquids due to a low surface wettability. Thus, to improve such processes a better understanding of the complex interplay between surface structure and wettability is needed. Therefore, we investigated the droplet impact onto a stand-alone cubic surface element, which represents one elementary aspect of the problem. To begin with, we performed a combined numerical/experimental study of the impact process on a stand-alone cubic pillar of 1 mm edge length, whose surface satisfied full wetting conditions [4]. The study showed a very good agreement between the droplet impact morphologies and also unravelled the process of air entrapment underneath the droplet, which can lead to the formation of one or multiple bubbles.

A brief literature review showed, that the experimental investigation of Juarez et al. [3] on a droplet impacting onto target posts with varying geometry (cylinders and polygons) comes closest to our experiments. The authors used water-glycerol droplets with a diameter of 2.85 mm and an impact velocity of 1.56 m/s, which results in a Weber number of $We = 250$ comparable to our experiments. The cross-sectional impact surface is kept constant for all post geometries and it equals the cross-sectional area of the impacting droplet. Juarez et al. [3] showed

that under identical impact conditions droplet splashing can be controlled by varying the cross-sectional geometry of the target post. For a cylindrical post geometry, a circular lamella spreading is observed, while for polygon targets (with vertices between $3 \leq n < 8$) the shape of the spreading lamella resembles the target cross-section rotated by an angle of π/n with respect to the target orientation [3]. At later times after impact, they observed the formation of filaments subsequent to the breakup of the lamella rim. For $3 \leq n \leq 8$ vertices, the number of filaments equals the number of target vertices, while for the cylindrical post and the target posts with more than 8 vertices, the filament number is independent of the target shape. However, the breakup processes of the lamella for cylindrical and high number vertices post proceeds in a similar fashion. The splashing behaviour can be also distinguished into two regimes: regular splashing for $3 \leq n \leq 8$ vertices and irregular splashing for cylindrical and $n \geq 8$ vertices target posts.

In this paper, we extend our previous investigation (Ren et al. [4]) by varying the edge length of the cubic pillar between 1 mm and 2.4 mm as well as its surface wettability (full wetting to almost non-wetting conditions). The parameter variation also includes multiple droplet diameters, impact velocities and two fluids, namely water and isopropanol. The droplet impact process is visualized with the multi-perspective experimental facility [2], that employs the total internal reflection-configuration to resolve the liquid-solid contact area. The goal is to gain a better understanding how the pillar size with respect to the droplet diameter affects the impact morphology and splashing behaviour. Furthermore, the effect of surface wettability is considered, to gain a better understanding of its interplay with surface structures.

Experimental method

The impact of a droplet onto a single, free-standing pillar with varying size is investigated experimentally with a multi-perspective (top, bottom, lateral and spatial view) imaging approach, see Figure 1. The corresponding test facility is only briefly described here. For detailed information on the facility and the post-processing procedures, please refer to the publication by Foltyn et al. [2]. The facility consists of the four main components: droplet generation unit, surface specimen, image acquisition unit, and the triggering and synchronisation unit. The droplet is generated with a "dropper". The liquid, fed by a syringe pump, accumulates at the tip of a blunt tilted needle and drips off in a regular manner. One random droplet is selected to pass to the droplet barrier and hits the surface specimen. The impact velocity of the droplet is selected by adjusting the droplets falling height. The surface specimen, i.e. the free-standing pillars, are made of acrylic glass. The pillar dimensions comply very well with the predefined edge lengths between 1 mm and 2.4 mm. The pillar base has a small radius of about 0.1 mm with

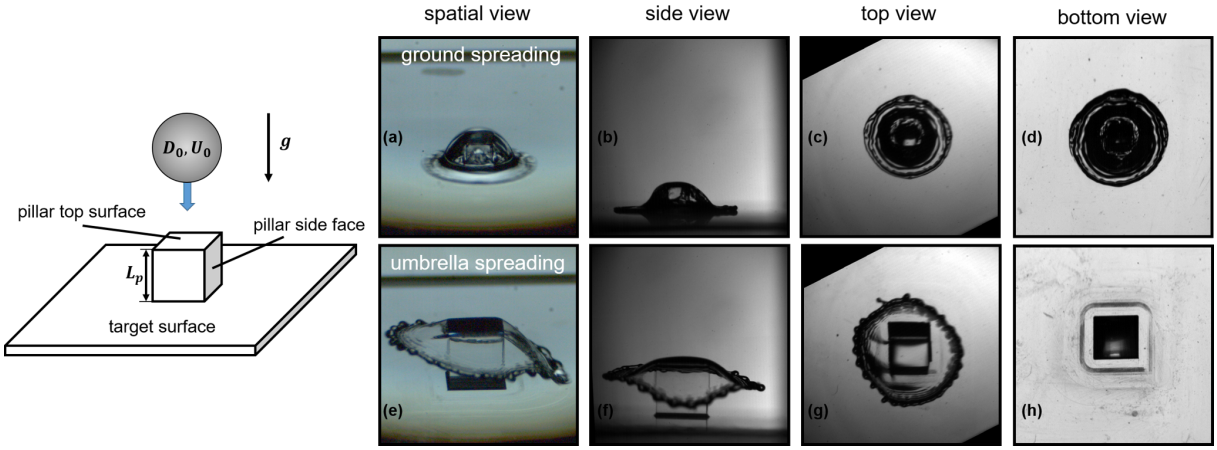

Figure 1. Sample images captured with the multi-perspective test-facility: upper row shows ground spreading at $t = 4$ ms (1 mm pillar edge length, $We = 180$) from a) spatial view, b) side view, c) top view and d) bottom view perspectives; lower row depicts umbrella spreading at $t = 3.6$ ms (pillar edge length of 2.4 mm, $We = 182$) from e) spatial view, f) side view, g) top view and h) bottom view perspectives.

respect to the surrounding flat surface, due to the manufacturing process. The experiments, however, confirmed that there is no significant influence on the impact morphology. The wetting behaviour of the surface specimen was manipulated using two different plasma treatments. Low pressure plasma activation was applied to improve the wetting behaviour, i.e. to reduce the contact angle. On the other hand, plasma polymerization was used to reduce the wetting behaviour and increase the contact angle. Hereby, the surface is coated with a very thin layer of high-molecular products, which does not interfere with the optical set-up. A detailed description of the plasma treatments is provided in Foltyn et al. [2]. The multi-perspective high-speed image acquisition comprises three different imaging techniques. The classical diffuse back-light imaging technique is used to record the lateral and top view perspectives of the droplet impact, see Figure 1 b, c, f, g. The top view is record at an angle of 13.4° to avoid an obstruction of the image by the dropper exit. The bottom view, shown in Figure 1 d, h, employs the total internal reflection method [1, 5], which allows to distinguish dry and wetted areas on the target surface. The fourth perspective is a spatial view that records a three-dimensional impression of the impact scenery (see Fig. 1 a, b). All cameras are triggered with a LASER light barrier, which the droplet passes before impact. The three main perspectives (top, bottom and lateral view) are recorded by two fully synchronised Photron SA-X2 cameras. One camera acquires the top and lateral view, while the second camera records the bottom view. The applied resolution for both cameras is 1024 × 672 px^2 at a frame rate of 20,000 fps (shutter speed: 1/88888 s). The utilised optical resolutions are 17 μm/px,18 μm/px, and 28 μm/px for the bottom, lateral, and top view, respectively. The spatial view is recorded with a Chronos 1.4 colour high-speed camera, which has a resolution of 1280 × 1024 px^2 at frame rate of 1,000 fps (shutter speed: 115.5 μs). The optical resolution of the spatial view is 11 μm/px. The Chronos camera is triggered simultaneously, but its recording is not synchronised with the Photron cameras. Each recorded image of the top, bottom and lateral views are individually corrected using previously acquired calibration measurements and bi-cubic interpolations to avoid any perspective distortion. Employing the image processing routine of Foltyn et al. [2], the droplet diameter and impact velocity are determined with an accuracy of 3.8% (2σ) and 1.3% (2σ), respectively. This results in an uncertainty of the Weber numbers of 4.6%.

Results and Discussion

The present study focuses on the impact of distilled water and isopropanol droplets onto a stand-alone cuboid with varying edge length of 1 mm, 1.6 mm, 2 mm and 2.4 mm, respectively. In addition to its size, also the wettability of the cuboid is varied. For both liquids fully wetting conditions ($\theta \approx 0°$) are achieved by plasma activation of the surface. On the other hand, plasma polymerization was used to reduce the wetting behaviour and to increase the contact angle for water to $\theta_{H_2 0} \approx 73.7°$ and for isopropanol to $\theta_{iso} \in [69°, 71°]$. The variations in droplet diameter and impact velocity are summarized in Table 1, together with the physical properties of the liquids. Note that, for water droplet impact onto the polymerized pillars an additional impact velocity of $3.35\ \mathrm{m\ s}^{-1}$ was investigated. In total, 65 experiments were performed from which here only droplet impacts in the vicinity of the pillar centre are discussed, while off-centre impacts are not considered.

First of all, the effect of pillar size on the droplet impact morphology is discussed. As shown in Figure 2, a change in pillar size from 1 mm edge length (Fig. 2a) to 2.4 mm (Fig. 2b) leads to a complete change of the liquids spreading behaviour. This is confirmed by the summary of observed impact morphology presented in Figure 3. As can be seen, the transition from ground to umbrella spreading always occurs at $\bar{L}_w \approx 0.83$ for water and $\bar{L}_{iso} = 1$ regardless of the employed Weber number and surface wettability. If the pillar edge length is smaller than the droplet diameter, hence the pillar length to droplet diameter ratio (pillar-drop ratio) is $\bar{L} = L_p/D_0 < 1$, *ground spreading* is observed. Hereby, the droplet liquid flows around the pillar, encloses it and spreads radially on the solid target surface, as shown in the centre row of Figure 2a. The wetting of the area directly surrounding the pillar is confirmed by the bottom view images (Fig. 2a,

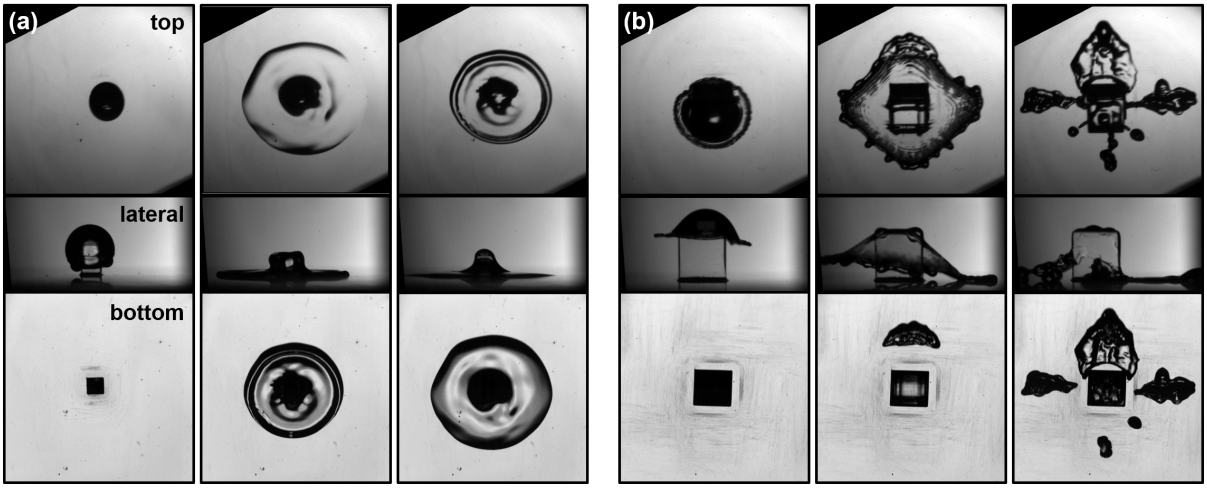

Figure 2. Top (upper row), lateral (centre row) and bottom perspective (bottom row) of water-droplet impact morphology: (a) ground spreading at full wetting conditions $\theta \approx 0$ with $We = 70$, pillar size 1 mm; (b) umbrella spreading at contact angle of $73.7°$ with $We = 180$, pillar size 2.4 mm.

bottom row), since here employing the total internal reflection method [1, 5] allows to distinguish unequivocally between dry and wetted areas. We already observed this impact morphology in our previous combined experimental and numerical study (Ren et al. [4]) for an isopropanol droplet impacting onto a pillar of 1 mm edge length ($\bar{L} = 0.5$). The liquid spreading around the cuboid entraps air at its four face sides. In the course of the impact process, the outer rim of the spreading liquid reaches the bottom wall and moves in both directions, towards the pillar foot as well as away from it. At the same time, fluid from the cuboid top starts to wet its vertical edges. Lastly, the droplet liquid also wets the pillars side faces, which leads to the formation of an air bubble, which is completely separated from the pillar sides [4]. In the present study, we observed this impact morphology also for water droplets and a pillar edge length of 1.6 mm, hence $\bar{L} \leq 0.8$.

If the pillar-drop ratio $\bar{L}$ exceeds 1, the spreading behaviour of the droplet proceeds differently, see Figure 2b. It starts on top of the pillar and proceeds in mid-air after the liquid leaves the pillars top surface. This behaviour is confirmed by the bottom view images. As shown in Figure 2b centre and bottom row, only the pillar top is wetted by the droplet liquid while the target surface around the pillar stays completely dry. The temporal evolution of this so-called *umbrella spreading* is shown in Figure 2b. As can be seen, almost no liquid flows along the pillar sides faces during the mid-air spreading. Eventually, due to gravity the liquid umbrella impacts onto

Table 1. Summary of the evaluated droplet impact parameters and the physical properties of the used liquids at an ambient temperature of $25°$ C.

	Distilled Water		Isopropanol (2-propanol)	
Droplet diameter	2.4 ± 0.024 mm		2.0 ± 0.020 mm	
Wetting condition	$\theta_{H_2O} \approx 0°$	$\theta_{H_2O} \approx 73.7°$	$\theta_{iso} \approx 0°$	$\theta_{iso} \in [69°, 71°]$
Impact velocity	1.45 m s^{-1}	1.45 m s^{-1}	1.49 m s^{-1}	1.49 m s^{-1}
	2.43 m s^{-1}	2.43 m s^{-1}	2.36 m s^{-1}	2.36 m s^{-1}
		3.35 m s^{-1}		
Density ρ	997.1 kg m^{-3}		781.5 kg m^{-3}	
Surface tension σ	0.07198 N m^{-1}		0.02092 N m^{-1}	
Dyn. viscosity μ	0.8897 mPa s		2.045 mPa s	

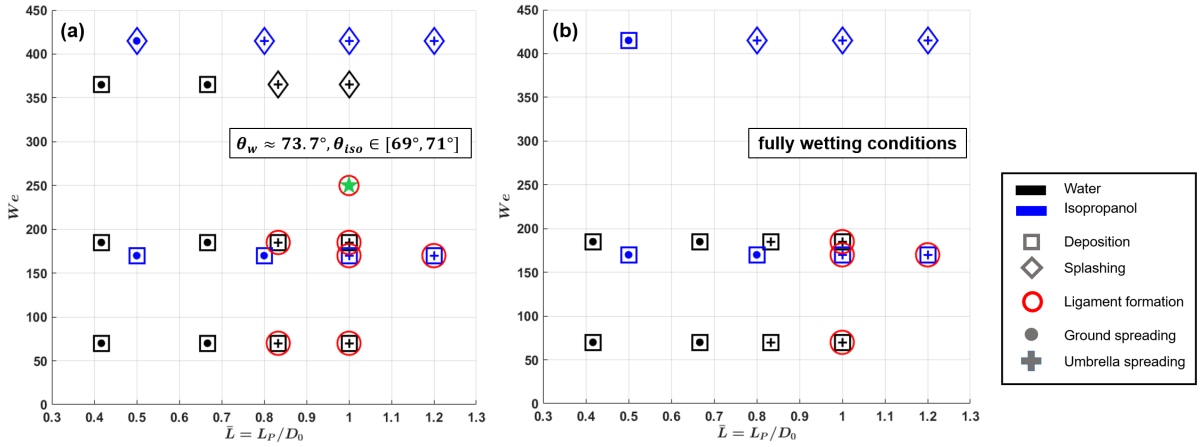

Figure 3. Summary of observed impact morphology as a function of Weber number We, $\bar{L} = L_p/D_0$ and surface wettability.

the target surface and is simultaneously ripped apart by the upper edges of the pillar. The umbrella spreading exhibits another distinguishing feature with respect to the ground spreading: the shape of the liquid lamella becomes rectangular. The corners of the lamella are azimuthally rotated by approximately 45° with respect to the pillar corners. Juarez et al. [3] reported the same behaviour for droplet impacts onto posts with cross-sectional polygon geometries with a number of vertices between $3 \leq n < 8$. The impact conditions were quite similar since they employed posts with an post-drop ratio of $\bar{L} = L_{post}/D_0 \approx 1$, water-glycerol droplets and an impact Weber number of $We_{Jua} = 250$. They also observed the formation of filaments subsequent to the breakup of the lamella rim. For $3 \leq n \leq 8$ target vertices, the same number of filaments are formed. In our study, we observe this filament formation, too. But instead of a mid-air filament formation, we observe it on the solid surface, see Figure 2b. Therefore, the filament formation seems to be strongly affected by the surface wettability. It is more pronounced for the surfaces with higher contact angles of $\theta \in [69°, 70°, 73.7°]$. Here the filaments remain intact after the spreading process is finished. In contrast, fully wetting conditions lead to a dissolving of the filaments. This can be seen also in Figure 3 where the impact morphology as a function of the pillar length to droplet diameter ratio $\bar{L}$, Weber number We and surface wettability is summarized. Here, the cases where filament formation was observed are marked by a red circle. As can be seen, the cases with ligament formation are more sparse for fully wetting conditions. An increase in wettability also seems to shift the occurrence of umbrella spreading to larger $\bar{L}$. Furthermore, Figure 3 confirms that the transition from ground to umbrella spreading is triggered mainly by the $\bar{L}$-value, while surface wettability, Weber number and liquid properties seem to have only a minor effect.

Finally, the transition from deposition to splashing is discussed briefly. In general, regular splashing was observed for cases that exhibit umbrella spreading and Weber numbers larger than $We > 350$. Also surface wettability effects the impact outcome: for isopropanol droplet impacts onto the smallest pillars ($\bar{L} = 0.5$), a fully wettable surface suppresses splashing.

Summary and Conclusion

In this paper, we investigated experimentally a single droplet impact onto a stand-alone cuboid with varying edge length between 1 mm and 2.4 mm in order to gain a better understanding of the complex interplay between surface structure and wettability, which is ubiquitous in nature and technology. Besides the cuboid size, the surface wettability and the droplet parameters, namely diameter, impact velocity and liquid properties, were varied. We found that an increase in pillar size, with respect to the droplet diameter, leads to a change in spreading morphology from *ground spreading* to *umbrella spreading*. Ground spreading is characterized by the spreading of the liquid lamella on the solid surface around the pillar, while umbrella spreading refers to the formation of the liquid lamella in mid-air. Umbrella spreading exhibits a unique

feature: a rectangular spreading shape, where lamella corners are azimuthally rotated by 45° with respect to the pillar corners. At later times after impact, ligament formation at the lamella corners is observed. The wettabilities investigated here showed only a minor effect on the spreading behaviour and the occurrence of splashing. The latter is observed for cases exhibiting umbrella spreading at $We > 350$. Our investigation revealed some new insights into the droplet impact behaviour on stand-alone cubic surface structures. Nevertheless, we are still at the beginning to understand these impact dynamics. Therefore, we plan to continue our research in this area.

Acknowledgements
The authors would like to thank the Deutsche Forschungsgemeinschaft (DFG) for the financial support of the project GRK 2160 "Droplet Interaction Technologies" (DROPIT), under project number 270852890.

References

[1] N. R. Arnold Frohn. *Dynamics of Droplets*. Springer Berlin Heidelberg, 2000.

[2] P. Foltyn, D. Ribeiro, A. Silva, G. Lamanna, and B. Weigand. Influence of wetting behavior on the morphology of droplet impacts onto dry smooth surfaces. *Physics of Fluids*, 33(6):063305, 2021.

[3] G. Juarez, T. Gastopoulos, Y. Zhang, M. L. Siegel, and P. E. Arratia. Splash control of drop impacts with geometric targets. *Phys. Rev. E*, 85(026319), 2012.

[4] W. Ren, P. Foltyn, A. Geppert, and B. Weigand. Air entrapment and bubble formation during droplet impact onto a single cubic pillar. *Sci. Rep.*, 11(1):18018, 2021.

[5] M. A. J. van Limbeek, M. Shirota, P. Sleutel, C. Sun, A. Prosperetti, and D. Lohse. Vapour cooling of poorly conducting hot substrates increases the dynamic Leidenfrost temperature. *International Journal of Heat and Mass Transfer*, 97:101–109, 2016.